UDC 66.067.38
DOI 10.12737/1560

INTENSIFICATION OF ULTRAFILTRATION CONCENTRATING BY THE SEPARATION OF THE CONCENTRATION BOUNDARY LAYER

B. A. Lobasenko[1] and A. G. Semenov[2]

Kemerovo Institute of Food Science and Technology,
bul'v. Stroitelei 47, Kemerovo, 650056 Russia
[1]phone/Fax: +7(3842) 39-68-42, e-mail: lobasenko@mail.ru
[2]phone/Fax: +7(3842) 68-00-49, e-mail: agsem55@yandex.ru

(Received January 10, 2013; Accepted in revised form February 11, 2013)

Abstract: The possibility of intensifying the ultrafiltration concentrating of food substance solutions by the separation of the near-membrane flow part that comprises the concentration boundary layer (or diffusion layer) enriched by a useful component has been investigated in this study. A mathematical model of the longitudinal development of polarization on a membrane with consideration of its selectivity (rejection coefficient) has been proposed. The efficiency of the separation of the near-membrane layer has theoretically been estimated on the basis of this model. Some constructions of membrane modules with the separation of the near-membrane layer have been proposed. Experiments have shown that the proposed method allows the concentrate to be enriched in the continuous-flow module by 9–10%, which is much higher than for the traditional concentrating process. The calculated concentration coefficients are in good agreement with experimental values.

Key words: ultrafiltration, concentrating, intensification, concentration polarization, rejection coefficient, concentration coefficient.

INTRODUCTION

The development of simple and economical methods for the separation, purification, and concentrating of liquid media is one of the most important problem in the food industry and, especially, in the dairy industry. Membrane technologies, which have a number of advantages in comparison with traditional separation methods, are especially noteworthy [1, 2]. This explains a profound interest in membrane processes, to which a considerable number of theoretical and experimental studies have been devoted.

However, membrane methods have some disadvantages reducing the efficiency of the process. The most essential of them is the formation of the diffusion boundary layer with an increased concentration of rejected substances on the membrane surface (i.e. concentration polarization), which promotes the formation of a gel layer hindering the removal of a solvent.

The weakening of concentration polarization is a traditional way of increasing the efficiency of membrane equipment [3]. It is attained via the turbulization of a flow with mechanical turbulizers [4–7] or gas sparging [9–13] or via the physical effect on a flow with mechanical vibrations [14–16], ultrasound [17–20], or an imposed electrical field [21]. All these methods lead to additional expenditures, complicate the structure of an apparatus, degrade the quality of a processed product, and increase its cost.

In this work, we consider the possibility of the intensification of ultrafiltration concentrating by the separation of the near-membrane part of a solution flow as a resulting product. It comprises the diffusion boundary layer, the concentration in which is appreciably higher than in the major part of a flow (flow middle). This enables the obtaining of a highly concentrated product at lower energy consumption, since a solution flows in the laminar regime.

The objective of our work is to perform the theoretical and experimental analysis of the efficiency of the separation of the near-membrane layer, to estimate the effect of geometrical and regime parameters, and to describe the technical implementation of the proposed idea.

OBJECTS AND METHODS OF STUDY

In the theoretical part of our work, we consider the mathematical model of the ultrafiltration concentrating of a high-molecular substance through a tubular membrane with a radius R, with the separation of the near-membrane flow part at the outlet of the membrane channel. In our analysis, we have made the following assumptions:

(1)A solution flows in the laminar regime, and the tangential velocity profile $u(r)$ is determined by the Hagen–Poiseuille equation

$$u(r) = 2U\left(1 - \frac{r^2}{R^2}\right), \qquad (1)$$

where r is the radial coordinate counted from the axis of the membrane channel, and U is the average velocity of a solution flow;

(2)The physical properties of a solution are constant and independent of the concentration of a high-molecular substance;

(3)The concentration of a high-molecular substance in the flow middle outside the diffusion layer is constant and equal to c_0;

(4)The thickness of the diffusion layer is much smaller than the radius of a membrane;

(5)The selectivity of a membrane with respect to the a filtered high-molecular substance is characterized by a constant rejection coefficient

$$\sigma = 1 - \frac{c_{per}}{c_{ret}}, \qquad (2)$$

where c_{per} is the concentration of a high-molecular substance in the permeate (the solution that has been passed through a membrane), and c_{ret} is the concentration of a high-molecular substance in the retentate (the solution rejected by a membrane) immediately near the surface of a membrane; and

(6)The possible decrease of the efficiency of a membrane is due to the formation of a gel layer on its surface, and the formation of a gel begins, when a certain solution concentration c_g is attained.

To model the development of polarization, we selected the integral method, which allows us to obtain simple and easily analyzable approximate estimates of the process characteristics.

The experimental studies of the process of concentrating were performed on the setup schematized in Fig. 1.

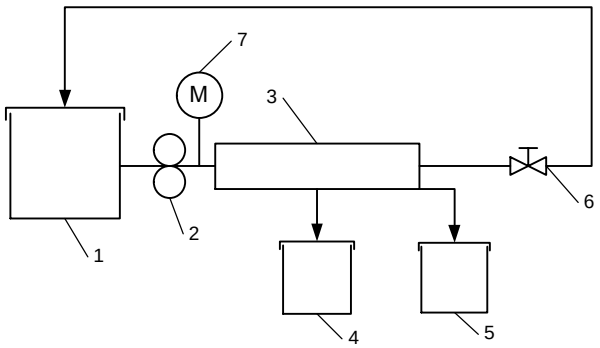

Fig. 1. Laboratory bench scheme: (*1*) initial solution vessel, (*2*) pump, (*3*) membrane module, (*4*) permeate collection vessel, (*5*) withdrawn concentrate collection vessel, (*6*) valve, (*7*) manometer.

Skim milk and dairy whey with a total solids content of 8.4 and 4%, respectively, were used as objects of experimental study. Tubular ceramic membranes of the two types, namely, aluminum oxide membranes with an average pore size of 20 nm (Mendeleev Russian University of Chemical Technology, Moscow) and silicon carbide membranes with an average pore size of 200 nm ("Ceramic Filter" Research and Production Association, Moscow) were applied for concentrating.

THEORETICAL ANALYSIS

1.1.Model of the Development of Concentration Polarization

Since the thickness of the diffusion layer is assumed to be small in comparison with the radius of a membrane, the surface curvature may be neglected. Then the flow of a solution and the mass transfer in the diffusion boundary layer can be described by the equations of a flat boundary layer

$$\begin{cases} \dfrac{\partial u}{\partial x} + \dfrac{\partial u}{\partial y} = 0, \\ u\dfrac{\partial c}{\partial x} + v\dfrac{\partial c}{\partial y} = D\dfrac{\partial^2 c}{\partial y^2}, \end{cases} \qquad (3)$$

with the boundary conditions

$$\left.\begin{array}{l} u = 0 \\ v = -J \\ \left(D\dfrac{\partial c}{\partial y} + \sigma J c\right)_{y=0} = 0 \end{array}\right\} \ (y = 0)\ ; \qquad (4)$$

$$\left.\begin{array}{l} u \to U \\ v \to 0 \\ c \to c_0 \end{array}\right\} \ (y \to \infty).$$

Here, x and y are the longitudinal coordinate and the coordinate orthogonal to the surface of a membrane ($y=R-r$), respectively, u and v are the longitudinal and transversal components of the velocity vector, c is the concentration of a high-molecular substance, D is the diffusion coefficient of a high-molecular substance, and J is the permeate flux, m^3/m^2s (or m/s).

From Eqs. (3) one can obtain

$$\begin{cases} (c - c_0)\left(\dfrac{\partial u}{\partial x} + \dfrac{\partial u}{\partial y}\right) = 0, \\ u\dfrac{\partial (c - c_0)}{\partial x} + v\dfrac{\partial (c - c_0)}{\partial y} = D\dfrac{\partial^2 (c - c_0)}{\partial y^2} \end{cases},$$

Summing these two equations and integrating the obtained relationship across the diffusion layer with consideration for boundary conditions (4), one obtains the integral equation

$$\frac{d}{dx}\left[\int_0^{\delta} u(c - c_0)dy\right] = J\left[c_0 - (1-\sigma)c_w\right], \qquad (5)$$

Here δ is the thickness of the diffusion layer, and the subscript w hereinafter means that the value of the parameter is taken on the surface of a membrane.

To obtain the approximate solution of Eq. (5), the velocity and concentration distributions within the diffusion layer are approximated by the expressions

$$c = c_0\left[1+\left(1-\frac{y}{\delta}\right)^2\right], \quad u(y)=\frac{4U}{R}y, \quad (6)$$

The linear approximation of the velocity distribution is used in compliance with the assumption about a small thickness of the diffusion layer taking into account Hagen–Poiseuille equation (1).

Using the variables

$$\xi=\frac{1}{16}\frac{x}{R}\cdot\left(\frac{J}{U}\right)^3\cdot Pe_D{}^2, \quad \eta=\frac{y}{\delta}, \quad \theta(\xi,\eta)=\frac{c-c_0}{c_0}, \quad p(\xi)=\frac{J\delta}{D}, \quad (7)$$

where $Pe_D=2UR/D$ is the diffusion Peclet number, and Eq. (6), Eq. (5) may be transformed into the dimensionless form

$$\frac{d}{d\xi}\left[p^2\theta_w\int_0^1\eta(1-\eta)^2d\eta\right]=1-(1-\sigma)(1+\theta_w), \quad (8)$$

In terms of variables (7), boundary condition (4) for the concentration on the surface of a membrane takes the form

$$\left(\frac{\partial\theta}{\partial\eta}\right)_w+p\sigma(1+\theta_w)=0$$

The derivative in this expression is determined from approximate equation (6) written in terms of variables (7). After simple rearrangements, one can obtain

$$\theta_w=\frac{p\sigma}{2-p\sigma}, \quad (9)$$

Substituting this expression into Eq. (8) and calculating the integral, we finally obtain the following differential equation for the dimensionless thickness of the diffusion layer p:

$$\frac{d}{d\xi}\left[\frac{p^3}{2-\sigma p}\right]=12\frac{2-p}{2-\sigma p}, \quad (10)$$

The initial condition for Eq. (10) has the form $p(0) = 0$.

In the case of an ideal membrane ($\sigma = 1$), Eq. (10) can be integrated. As a result, one obtains the cubic equation

$$p^3+12\xi\cdot p-24\xi=0, \quad (11)$$

the solution of which gives us the following expression for the immediate estimation of the dimensionless diffusion layer thickness:

$$p=\sqrt[3]{4\xi\left(3+\sqrt{4\xi+9}\right)}+\sqrt[3]{4\xi\left(3-\sqrt{4\xi+9}\right)}, \quad (12)$$

The dimensionless concentration of a high-molecular substance on the surface of a membrane is determined from Eq. (9).

In the general case, it is necessary to solve Eq. (10) numerically. The analysis of the solutions obtained at σ=0.5–0.9 shows that the distributions of the dimensionless diffusion layer thickness and high-molecular substance concentration can rather precisely be approximated by the formulas

$$p\approx\frac{2\xi^{0.723-0.190\sigma}}{0.098+0.122\sigma+\xi^{0.723-0.190\sigma}},$$

$$\theta_w\approx\frac{\sigma\xi^{0,723-0,190\sigma}}{(0.098+0.122\sigma)+\xi^{0.723-0.190\sigma}(1-\sigma)}, \quad (13)$$

If the gel forming concentration c_g is known, the corresponding dimensionless concentration θ_g can be found from Eq. (7). From Eq. (13) one obtains the formula for the cross section coordinate (the distance from the leading edge of a membrane), at which the formation of a gel begins:

$$\xi_g=\left[\frac{\theta_g(0.098+0.122\sigma)}{\sigma(1+\theta_g)-\theta_g}\right]^{\frac{1}{0.723-0.190\sigma}}, \quad (14)$$

It follows from Eq. (14) that the coordinate of the beginning of gel formation grows with a decrease in the rejection coefficient of a membrane.

1.2.Estimating the Parameters of the Separation of the Near-Membrane Layer

The constructed model for the development of polarization allows of the estimation of the possibility of the intensification of membrane concentrating by withdrawing the solution from the peripheral flow zone adjacent to the surface of a membrane.

To estimate the parameters of the partial withdrawal of the solution from the near-membrane zone, let us divide the flow that moves through a tubular membrane with a radius R, into the two parts, namely, the middle with a radius r^* and the peripheral part (concentrate) that flows through the annular cross section with an inner radius r^* and an outer radius R (Fig. 2). The volumetric concentrate flux through the cross section of the annular zone is

$$Q_{conc}=2\pi\int_{r^*}^{R}ru(r)dr, \quad (15)$$

Taking into account Hagen–Poiseuille equation (1), formula (15) can be written as

$$Q_{conc}=4\pi\cdot U\int_{r^*}^{R}\left(1-\frac{r^2}{R^2}\right)\cdot rdr=\pi R^2U\left[1-\left(\frac{r^*}{R}\right)^2\right]^2, \quad (16)$$

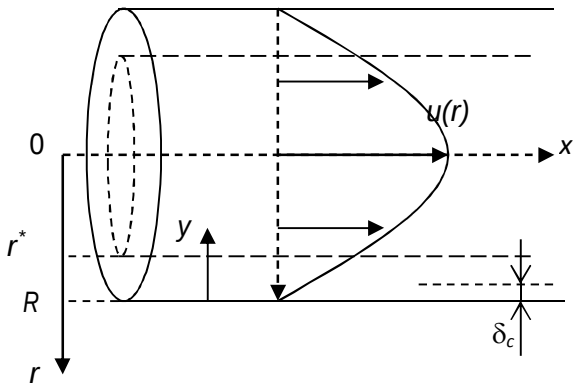

Fig. 2. Separation of the flow of a solution in a tubular membrane.

The mass flux of a dissolved high-molecular substance through the cross section of the annular zone is

$$G_{conc} = 2\pi \int_{r^*}^{R} u(r) \cdot c(r) \cdot r dr$$

Rearranging this expression into the form

$$G_{conc} = 2\pi \int_{r^*}^{R} u(r)(c - c_0) r dr + 2\pi \int_{r^*}^{R} u(r) c_0 r dr$$

and taking into account Eq. (15), one obtains

$$G_{conc} = 2\pi \int_{r^*}^{R} u(c - c_0) r dr + c_0 Q_{conc} \quad (17)$$

,

Taking into account that the concentration $c = c_0$ everywhere outside the diffusion layer with a thickness δ, this expression can be written as

$$G_{conc} = 2\pi \int_{r^*}^{R-\delta} u(c - c_0) r dr + 2\pi \int_{R-\delta}^{R} u(c - c_0) r dr +$$

$$+ c_0 Q_{conc} = 2\pi \int_{R-\delta}^{R} u(c - c_0) r dr + c_0 Q_{conc}, \quad (18)$$

Taking into consideration that the thickness of the diffusion layer is small, we can assume that $r \approx R$ and neglect the surface curvature. Introducing the variable $y = R - r$, one can write

$$\int_{R-\delta}^{R} u(c - c_0) r dr = R \int_{0}^{\delta} u(c - c_0) dy.$$

Passing to dimensionless variables (7) and taking into account Eq. (6), one obtains in Eq. (18)

$$G_{conc} = c_0 Q_{conc} + 2\pi R \int_{0}^{\delta} u(c - c_0) dy = c_0 Q_{conc} + 8\pi U c_0 \delta^2 \int_{0}^{1} \theta \eta d\eta.$$

Taking into account Eqs. (6), (7), and (9), the high-molecular substance mass flux through the cross section of the peripheral annular zone is finally determined by the expression

$$G_{conc} = c_0 Q_{conc} + 2\pi U c_0 \delta^2 \frac{p\sigma}{3(2 - p\sigma)}. \quad (19)$$

Dividing this expression by Eqs. (16), one obtains the average concentration of the concentrate withdrawn from the peripheral zone as

$$c_{conc} = c_0 \left[1 + \frac{2 p\sigma\delta^2}{3(2 - p\sigma)\left(1 - \frac{r^{*2}}{R^2}\right)^2 R^2} \right], \quad (20)$$

Let us introduce the parameters

$$\left(\frac{r^*}{R}\right)^2 = \Phi < 1, \qquad Pe_J = \frac{2JR}{D}, \quad (21)$$

and the dimensionless concentration coefficient K determined as the ratio of the average concentration in the withdrawn peripheral flow part to the initial concentration c_0. The concentration coefficient is expressed from Eq. (20) with consideration for Eqs. (7) and (21) as

$$K = \frac{c_{conc}}{c_0} = 1 + \frac{8}{3 Pe_J^2 (1 - \Phi)^2} \left(\frac{p^3 \sigma}{2 - p\sigma} \right), \quad (22)$$

The concentration coefficient value allows the estimation of the possibility of obtaining an enriched solution via the separation of its peripheral part.

CONCENTRATE SEPARATION DEVICES

A number of devices have been developed for the technical implementation of the idea of the processed solution withdrawal from the near-membrane zone. One of them [22] is shown in Fig. 3.

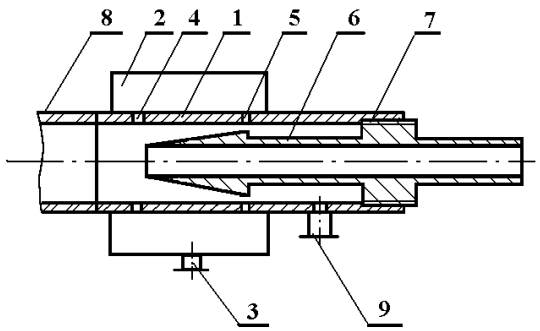

Fig. 3. Device for the separation of the near-membrane layer: (*1*) housing, (*2*) shell, (*3*), (*9*) fittings, (*4*), (*5*) slots, (*6*) rod, (*7*) thread, (*8*) tubular membrane.

The device operates as follows. The initial solution is subjected to filtration, being passed though tubular membrane *8* under pressure. A layer with an increased concentration of dissolved substances is formed near the inner surface of the membrane. The flow enters housing *1* with two annular slots *4* and *5*. The pressure created in the first of them is higher than the pressure in the second slot. The pressures are adjusted by displacing the conical tip of hollow rod *6*.

The pressure created in shell *2* is lower than the pressure in the cross section of slot *4* (but it is higher than in the cross section of slot *5*). As a result, the solution layer part adjacent to the inner housing surface is sucked into the shell and then removed through fitting *3*. The remaining flow is divided by the conical tip of the hollow rod into the two parts: the near-wall layer and the middle. The near-wall layer is passed between the rod and the housing and withdrawn trough fitting *9*. Hence, the concentrate can be withdrawn by the two ways, namely, though fittings *3* and *9*.

The middle, in which the concentration of a dissolved high-molecular substance is lower than its concentration in the concentrate, is withdrawn through the central channel of hollow rod *6*.

Another device [23], which enables the periodical mechanical cleaning of the membrane surface alongside with the withdrawal of the concentrate, is schematized in Fig. 4.

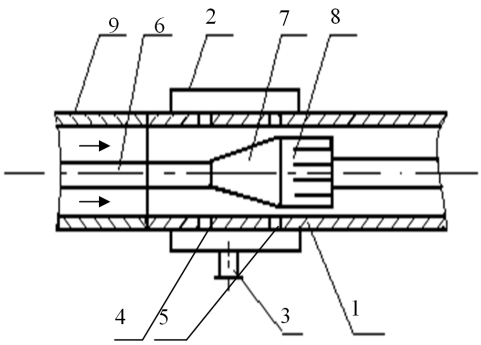

Fig. 4. Membrane module with devices for the withdrawal of the concentrate and the mechanical cleaning of a membrane: (*1*) housing, (*2*) shell, (*3*) fitting, (*4*), (*5*) annular slots, (*6*) guiding rod, (*7*) cone, (*8*) cleaning device, (*9*) tubular ceramic membrane.

The device consists of housing *1*, on which shell *2* with fitting *3* for the withdrawal of the concentrate are situated. The housing has two annular slots *4* and *5*. Guiding rod 6, on which cone 7 with cleaning device *8* representing a "skirt" of mobile blade scrapers, is enclosed inside the housing. The housing is attached to tubular membrane *9*.

The device operates as follows. The initial solution under pressure flows through tubular membrane *9*. The flow moves into housing *1* with annular slots *4* and *5*. Due to conical attachment *7*, the pressure in the region of slot *5* is lower than in the region of slot *4*. Due to this factor, the intermediate pressure less than the pressure in the region of slot 4 is maintained inside shell *2*. As a result of this, the concentrate layer is sucked from the near-wall flow zone into the shell, from which it is removed through fitting 3, due to the pressure drop between the cross section of slot *4* and shell *2*. The process is controlled by adjusting the pressure in shell *2*. The middle is passed between the cone and the housing and then withdrawn from the module.

In the course of filtration, the blades of the cleaning device are arranged by the flow of a solution in parallel to it and do not hinder its motion.

To clean the membrane, the direction of the flow should be switched. The cone opening and the cleaning device move along guiding rod *6* and the membrane under the action of the reverse flow of a solution. The cleaning device blades are unfolded and forced against the inner surface of the membrane, thus removing the deposit layer. After the cone has passed along the membrane, the direction of the flow is switched again, and the cone and the cleaning device are returned into the initial position. If necessary, the operation of cleaning is repeated several times.

II. RESULTS AND DISCUSSION

2.1.Theoretical Results

The estimation of the diffusion layer thickness according to Eq. (13) shows that the change of the membrane rejection coefficient has a slight effect on the dimensionless layer thickness *p* (Fig. 5).

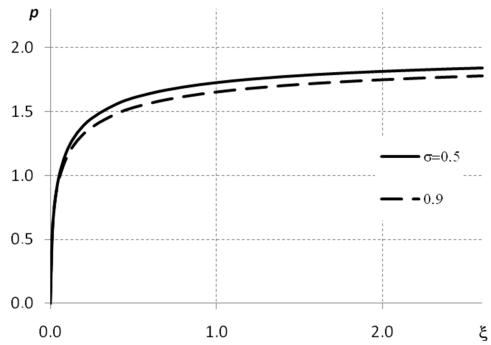

Fig. 5. Effect of the membrane rejection coefficient on the diffusion layer thickness.

At the same time, the change of the rejection coefficient has a considerable effect on the surface solution concentration distribution, which determines the beginning of the gel formation. The change of the excess dimensionless concentration θ_w along the membrane surface is illustrated in Fig. 6.

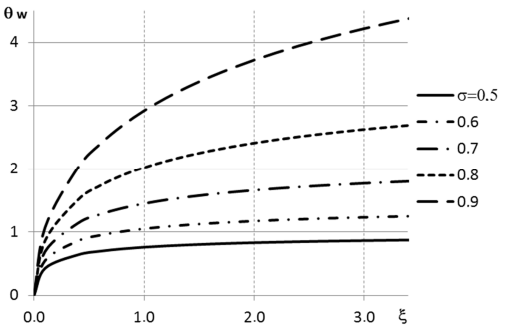

Fig. 6. Effect of the membrane selectivity on the distribution of surface concentrations.

It can be seen that a decrease in the membrane rejection coefficient reduces the surface concentration of a dissolved substance. This in turn delays the formation of a gel.

It should be noted that Eq. (13) implies the existence of the ultimate layer thickness and concentration at increasing membrane length, i.e.,

$$p \xrightarrow[\xi\to\infty]{} 2, \qquad \theta_w \xrightarrow[\xi\to\infty]{} \frac{\sigma}{1-\sigma}, \quad (23)$$

The ultimate thickness of the diffusion layer and the ultimate concentration of a dissolved substance near the surface of a membrane are determined from these expressions subject to Eq. (7) as

$$\delta_{\lim} = \frac{2D}{J}, \qquad c_{w\lim} = \frac{c_0}{1-\sigma}$$

The knowledge of these parameters allows us to estimate the danger of the fouling of a membrane due to the formation of a gel layer.

To estimate the efficiency of the withdrawal of the concentrate from the near-wall zone of the membrane channel, let us first consider the case of an ideal membrane with a rejection coefficient of 1. In this case, concentration coefficient expression (22) subject to Eq. (11) takes the form

$$K = 1 + \frac{32}{Pe_J^2 \left(1-\Phi\right)^2}\xi \quad (25)$$

Taking into account Eqs. (7) and (21), this expression can be written with the use of physical variables as

$$K = 1 + \frac{2}{\left(1-\Phi\right)^2}\left(\frac{x}{R}\frac{J}{U}\right) \quad (26)$$

From this formula it can be seen that the concentration coefficient grows with an increase in the permeate flux and a decrease in the tangential flow velocity. It grows as well with an increase in the parameter Φ (i.e., in the volume of the solution withdrawn as a concentrate). Moreover, the concentration coefficient grows linearly along the length of a membrane.

The results of calculating the concentration coefficient in compliance with Eq. (27) are plotted in Fig. 7.

In the case of the nonideal membrane (σ < 1), the concentration coefficient was calculated by approximate formulas (13). The results shown in Fig. 8 were obtained for the following conditions: membrane channel radius *R=2* mm; flow velocity *U*=0.12 m/s, permeate flux $J=1.39\cdot10^{-6}$ m/s, Φ=0.75, processed medium is skim milk.

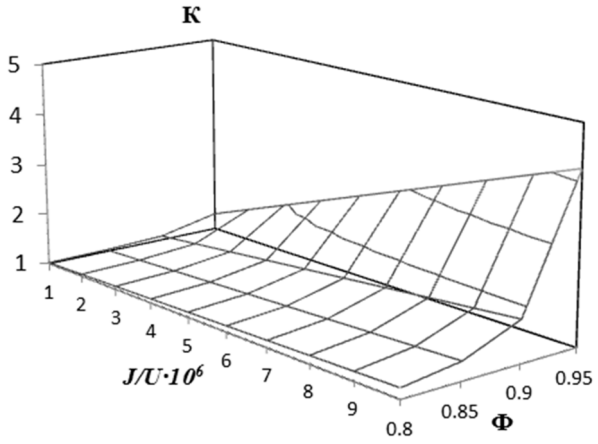

Fig. 7. Concentration coefficient of an ideal membrane for the separation of the near-wall flow part.

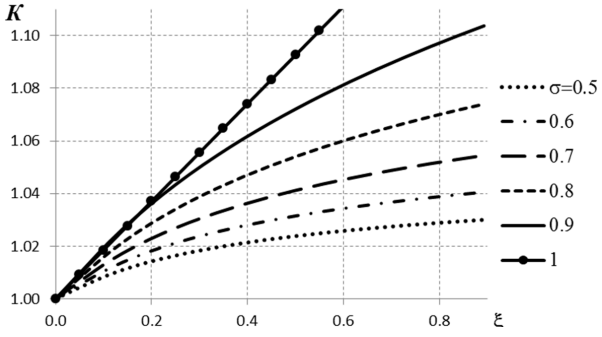

Fig. 8. Effect of the membrane rejection coefficient of the efficiency of concentrating.

As can be seen, the concentration coefficient grows with increasing distance from the leading edge of a membrane. The rate of its growth gradually decreases. It can be seen as well that the separation of the near-wall flow part, for example, at a membrane rejection coefficient of 0.7, allows us to attain a more than 5-% increase in the resulting product concentration in a continuous-flow membrane module with a dimensionless length ξ=0.8. This corresponds to the length of a tubular membrane of 0.72 m for the above conditions and the processing of skim milk.

2.2.Results of Experimental Studies

To confirm the possibility of the intensification of concentrating by the separation of the near-wall flow part, we performed some experiments on the concentrating of skim milk with an initial total solids content of 8.4%. A ceramic aluminum oxide membrane with a length of 800 mm, an inner diameter of 4 mm and an average pore diameter of 20 nm was used. The concentrate was separated using the device shown in Fig. 3.

The total solids contents in the concentrate obtained at different intensities of its withdrawal through fittings 3 and 9 (Fig. 3) are plotted in Fig. 9. The withdrawal intensities are given in l/h per 1 m^2 of the membrane surface.

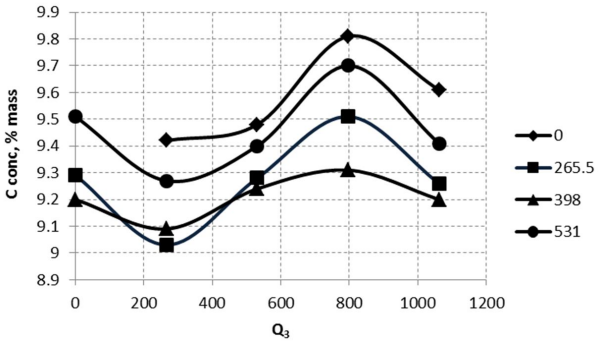

Fig. 9. Total solids content in the concentrate of skim milk (*p*=0.2 MPa, *Re* ≈ 2300).

The analysis of the given values shows that the total solids content in the concentrate lies within a range of 9–9.8% at different ratios of the intensities of its withdrawal through the fittings, thus corresponding to the concentration coefficient of 1.07–1.17. On the whole, this agrees with the estimates obtained with the model described above (Fig. 8).

We have also performed some experiments on the concentrating of skim milk (c_0 = 8.4%) and dairy whey (c_0 = 4.8%) using ceramic membranes of the two types: membranes with a pore size of 20 nm (Mendeleev Russian University of Chemical Technology, Moscow) and membranes with a pore size of 200 nm ("Ceramic Filter" Research and Production Association, Moscow). The concentrate was separated using the device shown in Fig. 4. The results are plotted in Fig. 10.

As one can see from Fig. 10, the separate withdrawal of the solution from the outlet of the membrane module in these experiments also leads to an appreciable increase in the total solids content of the concentrate in comparison with the initial solution. The highest concentration coefficient is 1.21 for skim milk and 1.17 for whey.

The total solids content of the concentrate decreases with increasing concentrate withdrawal intensity. This agrees with the modeling results. According to Eqs. (16) and (21), an increase in the amount of the withdrawn concentrate corresponds to a decrease in the parameter Φ. According to Eq. (22), this results in a decrease in the concentrate concentration coefficient.

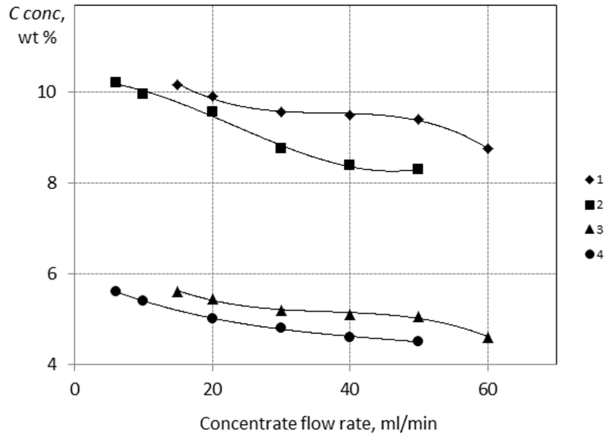

Fig. 10. Total solids content in the concentrate: (*1*), (*3*) on the membrane with 200-nm pores, (*2*), (*4*) on the membrane with 20-nm pores, (*1*), (*2*) the medium is skim milk, and (*3*), (*4*) the medium is dairy whey (*p* = 0.15 MPa, *t* = 20°C, *Re* ≈ 500).

As one can see from Fig. 10, the use of the membranes with greater pores (consequently, with a lower rejection coefficient) turned out to be more efficient from the viewpoint of increasing the concentration of the resulting product for both skim milk and dairy whey. This paradoxical result may be explained relying on the modeling results. Under all other conditions being equal, an increase in the pore size leads to the growth of the permeate flux due to a decrease in the hydraulic resistance of a membrane. Meanwhile, as one can see, for example, from Eq. (27), an increase in the permeate flux leads to the growth of the concentration coefficient. It may be supposed that the effect of the permeate flux change on the efficiency of concentrating has proven to be much more considerable in this case than the effect of the rejection coefficient of a membrane.

CONCLUSIONS

The obtained results indicate that the separation of the near-wall flow part in the membrane concentrating with the use of tubular membrane modules allow us to increase the concentration of the resulting product. This effect is attained even in the case of membranes with the partial rejection of a dissolved substance. This opens up the opportunity for intensifying the membrane processes of the processing of dairy raw materials.

REFERENCES

1. Brans, G., Schroen, C.G.P.H., van der Sman, R.G.M., and Boom, R.M., Membrane fractionation of milk: state of the art and challenges, *Journal of Membrane Science*, 2005, vol. 243, pp. 263–272.

2. Van Reis, R. and Zydney, A., Bioprocess membrane technology, *Journal of Membrane Science*, 2007, vol. 297, pp. 16–50.

3. Wakeman, R.J. and Williams, C.J., Additional techniques to improve microfiltration, *Separation and Purification Technology*, 2002, vol. 26, pp. 3–18.

4. Krstićś, D.M., Tekić, M.N., Carić, M.D., and Milanović, S.D., Static turbulence promoter in cross-flow microfiltration of skim milk, *Desalination*, 2004, vol. 163, pp. 297–309.

5. Pal, S., Bharihoke, R, Chakraborty, S., Ghatak, S.K., De, S., and DasGupta, S., An experimental and theoretical analysis of turbulence promoter assisted ultrafiltration of synthetic fruit juice, *Separation and Purification Technology*, 2008, vol. 62, pp. 659–667.

6. Popović, S. and Tekić, M.N., Twisted tapes as turbulence promoters in the microfiltration of milk, *Journal of Membrane Science*, 2011, vol. 384, pp. 97–106.
7. Zhou, N. and Agwu Nnanna, A.G., Investigation of hybrid spring-membrane system for fouling control, *Desalination*, 2011, vol. 276, pp. 117–127.
8. Popović, S., Jovičević, D., Muhadinović, M., Milanović, S., and Tekić, M.N., Intensification of microfiltration using a blade-type turbulence promoter, *Journal of Membrane Science*, 2012, vol. 425–426, pp. 113–120.
9. Taha, T. and Cui, Z.F., CFD modelling of gas-sparged ultrafiltration in tubular membranes, *Journal of Membrane Science*, 2002, vol. 210, pp. 13–27.
10. Mercier-Bonin, M., Gesan-Guiziou, G., and Fonade, C., Application of gas/liquid two-phase flows during crossflow microfiltration of skimmed milk under constant transmembrane pressure conditions, *Journal of Membrane Science*, 2003, vol. 218, pp. 93–105.
11. Psoch, C. and Schiewer, S., Dimensionless numbers for the analysis of air sparging aimed to reduce fouling in tubular membranes of a membrane bioreactor, *Desalination*, 2006, vol. 197, pp. 9–22.
12. Cheng, T.-W. and Li, L.-N., Gas-sparging cross-flow ultrafiltration in flat-plate membrane module: Effects of channel height and membrane inclination, *Separation and Purification Technology*, 2007, vol. 55, pp. 50–55.
13. Qaisrani, T.M. and Samhabe, W.M., Impact of gas bubbling and backflushing on fouling control and membrane cleaning, *Desalination*, 2010, vol. 266, pp. 154–161.
14. Akoum, O.Al., Jaffrin, M.Y., Ding, L., Paullier, P., and Vanhoutte, C., An hydrodynamic investigation of microfiltration and ultrafiltration in a vibrating membrane module, *Journal of Membrane Science*, 2002, vol. 197, pp. 37–52.
15. Akoum, O., Jaffrin, M.J., and Ding, L.-H., Concentration of total milk proteins by high shear ultrafiltration in a vibrating membrane module, *Journal of Membrane Science*, 2005, vol. 247, pp. 211–220.
16. Gomaa, H.G. and Rao, S., Analysis of flux enhancement at oscillating flat surface membranes, *Journal of Membrane Science*, 2011, vol. 374, pp. 59–66.
17. Kobayashi, T., Chai, X., and Fujii, N., Ultrasound enhanced cross-flow membrane filtration, *Separation and Purification Technology*, 1999, vol. 17, pp. 31–40.
18. Muthukumaran, S., Kentish, S.E., Ashokkumar, M., and Stevens, J.W., Mechanisms for the ultrasonic enhancement of dairy whey ultrafiltration, *Journal of Membrane Science*, 2005, vol. 258, pp. 106–114.
19. Kyllonen, H.M., Pirkonen, P., and Nystrom, M., Membrane filtration enhanced by ultrasound: a review, *Desalination*, 2005, vol. 181, pp. 319–335.
20. Cai, M., Zhao, S., and Liang, H., Mechanisms for the enhancement of ultrafiltration and membrane cleaning by different ultrasonic frequencies, *Desalination*, 2010, vol. 263, pp. 133–138.
21. Sarkar, B., Pal, S., Ghosh, T.B., De, S., and DasGupta, S., A study of electric field enhanced ultrafiltration of synthetic fruit juice and optical quantification of gel deposition, *Journal of Membrane Science*, 2008, vol. 311, pp. 112–120.
22. RF Patent 2181619, 2000.
23. RF Patent 2234360, 2004.